

# Extensions on low-complexity DCT approximations for larger blocklengths based on minimal angle similarity

A. P. Radünz\*    L. Portella\*    R. S. Oliveira\*    F. M. Bayer†    R. J. Cintra‡

## Abstract

The discrete cosine transform (DCT) is a central tool for image and video coding because it can be related to the Karhunen-Loève transform (KLT), which is the optimal transform in terms of retained transform coefficients and data decorrelation. In this paper, we introduce 16-, 32-, and 64-point low-complexity DCT approximations by minimizing individually the angle between the rows of the exact DCT matrix and the matrix induced by the approximate transforms. According to some classical figures of merit, the proposed transforms outperformed the approximations for the DCT already known in the literature. Fast algorithms were also developed for the low-complexity transforms, asserting a good balance between the performance and its computational cost. Practical applications in image encoding showed the relevance of the transforms in this context. In fact, the experiments showed that the proposed transforms had better results than the known approximations in the literature for the cases of 16, 32, and 64 blocklength.

## Keywords

Discrete cosine transform, fast algorithms, image compression, low-complexity transform

## 1 Introduction

Current technological trends suggest an ever-increasing demand for efficient, low-power, low-complexity digital signal processing methods [100, 28, 42, 111]. In this context, many important discrete transforms have become useful tools for signal coding and data decorrelation [34, 14, 67, 74, 82] such as the discrete Fourier transform (DFT), the discrete Hartley transform (DHT), the Walsh-Hadamard transform (WHT), the discrete Tchebichef transform (DTT), the discrete cosine transform (DCT), among others. Data compression techniques [43, 106, 71, 46] address the problem of removing redundancy from data [82, pg. 2]. Such removal can be accomplished by using the Karhunen-Loève transform (KLT) [67, 14], which is the optimal tool in terms of energy compaction. Indeed, the KLT packs the energy of the input signal in few transform-domain coefficients and diagonalizes the covariance or correlation matrix of the data, resulting in a completely decorrelated signal [67, pg. 10]. In practice, the KLT is not widely adopted because it is a data-dependent transformation, which severely precludes the development of fast algorithms. Fast algorithms can highly reduce the arithmetic cost of the transform since it searches for a computationally efficient way of implementing it [8, pg. 2].

However, if the input signal is a first-order Markovian process, then the KLT matrix depends only on the correlation coefficient  $\rho$  of the process. Natural images constitute a representative class of such kind of data,

\*Independent researcher, previously with the Universidade Federal de Pernambuco (UFPE), Recife, Brazil.

†Departamento de Estatística and LACESM, Universidade Federal de Santa Maria, Santa Maria, Brazil.

‡Signal Processing Group, Departamento de Tecnologia, UFPE, Caruaru, Brazil. E-mail: rjdsc@de.ufpe.br

which often present high values of  $\rho$ . When  $\rho \rightarrow 1$ , the KLT becomes the type-II discrete cosine transform which is independent of the input data or any other parameter [14, pg. 56]. Although natural images do not necessarily present  $\rho = 1$ , their correlation coefficient is sufficiently high [34] to make the DCT extremely efficient and popular in image and video coding, such as JPEG [103], MPEG [77], and HEVC [75]. Since its introduction in [1], the DCT has been shown to be a superior tool when compared to the other transforms known in the literature in this context of image and video coding. This fact was confirmed in a number of independent works such as [103, 23, 22, 43, 67, 14, 79, 34, 84, 80]. The fact that the DCT is data-independent allows the development of low-complexity fast algorithms for its calculation [8].

Nevertheless, under scenarios of severe restrictions on processing power or energy autonomy [21, 88], the arithmetic cost of computing the DCT by traditional algorithms might still be a hindrance. Thus, several multiplierless low-complexity DCT approximations have been developed as detailed in [38, 53, 20, 21, 11, 13, 96, 5, 26, 68]. Particularly, we separate the method presented in [68], where a DCT approximation is derived by minimizing the angle between each corresponding rows of the exact and approximate transforms. The resulting 8-point DCT approximation introduced in [68] outperforms well-known DCT approximations in the literature according to classical figures of merit as the mean squared error, total energy error, coding gain, and transform efficiency. Furthermore, the associated fast algorithm requires only 24 additions and 6 bit-shifting operations.

The search for 8-point DCT approximations is a relatively mature area of research since the 8-point DCT is a key block in many image and video processing applications. However, with the advancement of image and video encoding technology, there is a demand for larger blocklengths that could be employed in modern codecs [89]. For instance, there is a new video standard coding, the Versatile Video Coding (VVC) [112], that requires 64-point transforms. In this paper, we extended the method proposed in [68] for larger blocklengths, i.e., for  $N = 16, 32$ , and  $64$ . To the best of our knowledge, the current literature archives only a few works [13, 6, 27] addressing low-complexity approximations for the DCT of the above-mentioned sizes. We aim at proposing high-performing low-complexity DCT approximations for such blocklengths.

The paper is structured as follows. In Section 2, we present a brief review of the relevance of the DCT and approximations in the context of hardware implementation and its applications. In Section 3, we review the formulation of the DCT and low-complexity approximations. Section 4 presents the methodology for deriving the proposed transformations. In Section 5, the introduced DCT approximations are presented along with performance assessment and fast algorithms derivation. Section 6 presents computational experiments in image compression that demonstrate the suitability of the suggested tools. Section 7 concludes the paper.

## 2 Hardware review

The energy packing and high decorrelation properties for signals modeled after highly-correlated first-order Markovian process makes the DCT a widely employed method for image and video coding [79]. In this context, the DCT is the main tool [25, 17, 68, 24, 93, 109, 54, 70, 2], finding implementations in JPEG [76], motion JPEG [7], MPEG [15], and HEVC [91, 65, 62]. Such efficient encoders can provide a significant reduction in computational complexity, enabling the development of high-speed computing architecture [94]. Popular architectures that benefited from transform-based encoding include HD and UHD videos [90, 29], smart antenna applications [97, 59], secure image processing [78, 60], image fusion [35] and defusion [55], biomedical signal

processing [101, 102], to cite a few.

Therefore, the design of DCT-based very large-scale integration (VLSI) structures has been an essential task for decreasing chip area, power, and time consumption [18, 19, 41, 87]. Thus, resource-constrained platforms which require hardware designs capable of larger autonomy, increased storage capacity, extended battery life, and data transmission are prime beneficiaries of low-complexity methods. This is illustrated in the case of low-powered devices in real-time applications [83] and nanotechnologies [3], which require ultralow power consumption. In addition, sensor architectures that present stringent limitations on memory and processing speed [50, 66, 113] and sub-branches like approximate memory, which focus on the trade off between perfect data fidelity and storage density [56], received technical contributions from DCT approximations. The requirements for low-cost computation can be easily noticed in the context of Internet of Things (IoT) [16, 36, 57, 64] or 5G technologies [47, 72], for example. The assumption that approximate methods lead to hardware implementations of low resource consumption was corroborated in a comprehensive study detailed in [76].

Motivated by this increasing demand, we focus our work on further reducing the arithmetic complexity of the DCT computation, which directly affects hardware-oriented measures such as chip area, dynamic power consumption, critical path delay, gate-count, area-time, and maximum clock frequency (throughput) [49, 110, 93, 58, 44, 31, 98].

### 3 Exact and approximate DCT

The  $N$ -point DCT is represented by an  $N \times N$  matrix  $\mathbf{C}_N$  whose elements are given by [14, pg. 61]:

$$c_{i,j} = \sqrt{\frac{2}{N}} u_i \cos \left\{ \frac{i(2j+1)\pi}{2N} \right\}, \quad i, j = 0, 1, \dots, N-1, \quad (1)$$

where the quantities  $u_i$  are defined as:

$$u_i = \begin{cases} \frac{1}{\sqrt{2}}, & \text{if } i = 0, \\ 1, & \text{if } i \neq 0. \end{cases} \quad (2)$$

Let  $\mathbf{x} = [x_0 \ x_1 \ \dots \ x_{N-1}]^\top$  be an  $N$ -point input vector. The DCT transformation of  $\mathbf{x}$  is the output vector  $\mathbf{X} = [X_0 \ X_1 \ \dots \ X_{N-1}]^\top$ , given by  $\mathbf{X} = \mathbf{C}_N \cdot \mathbf{x}$ . Since the DCT matrix is orthogonal, its inverse transformation can be written as  $\mathbf{x} = \mathbf{C}_N^\top \cdot \mathbf{X}$  [14, pg. 41].

Generally, DCT approximations are transformations  $\hat{\mathbf{C}}_N$  that behave similarly to the exact DCT according to a relevant criterion depending on the context at hand. An approximate transform is usually based on a low-complexity transform  $\mathbf{T}_N$ , i.e., a transformation matrix whose entries possess very low multiplicative complexity [8, 14]. Typical examples of low-complexity multipliers are:  $\{0, \pm 1, \pm 2, \pm 4, \dots\}$ ,  $\{0, \pm \frac{1}{2}, \pm 1, \pm 2, \pm 3\}$ , and  $\{0, \pm \frac{1}{4}, \pm \frac{1}{2}, \pm 1\}$ ; in all the above cases, the multiplication of a given number by any set element requires no or a few additions and bit-shifting operations. Once a low-complexity matrix is obtained, we can derive the associate approximate transform according to the next formalism [21, 39]:

$$\hat{\mathbf{C}}_N = \mathbf{S}_N \cdot \mathbf{T}_N, \quad (3)$$

where

$$\mathbf{S}_N = \sqrt{[\text{diag}(\mathbf{T}_N \cdot \mathbf{T}_N^\top)]^{-1}}, \quad (4)$$

being  $\text{diag}(\cdot)$  the diagonal matrix generated by its arguments and  $\sqrt{\cdot}$  the matrix square root operator [39]. If  $\mathbf{T}_N$  is almost orthogonal [21], then the matrix  $\hat{\mathbf{C}}_N$  can represent a meaningful approximation for  $\mathbf{C}_N$ . The concept of almost orthogonality stems from almost diagonality property as defined in [33, 21].

Notice that if  $\mathbf{T}_N$  presents the property of diagonality ( $\mathbf{T}_N \cdot \mathbf{T}_N^\top = [\text{diagonal matrix}]$ ) than (3) provides an orthogonal approximation  $\hat{\mathbf{C}}_N$ . In addition, if  $\mathbf{T}_N$  is orthogonal than  $\mathbf{S}_N$  results in the identity matrix  $\mathbf{I}_N$  and  $\hat{\mathbf{C}}_N = \mathbf{T}_N$ .

However, finding a good low-complexity matrix  $\mathbf{T}_N$  can be a hard task, because of the large search space. For instance, the matrix space of  $16 \times 16$  low-complexity matrices defined over the set  $\{-1, 0, +1\}$  possesses  $3^{16^2} \approx 1.39 \times 10^{122}$  candidate matrices. An exhaustive search over this space would take approximately  $4.41 \times 10^{105}$  years of computation assuming that each matrix could be generated and assessed in 1 nanosecond.

Therefore, a crucial step in deriving approximations is the reduction of the search space by restricting the search to potentially good matrices only. Literature describes several methods to accomplish such reduction: (i) matrix quantization [82]; (ii) matrix parametrization [10, 51]; (iii) algorithm parametrization [32, 96]; and (iv) visual inspection [5, 11, 9, 12, 13, 37, 86]. Depending on the particular search space reduction approach, the number of candidate approximations can be as small as just one matrix (e.g., SDCT [38] and RDCT [20]) or as large as classes of various matrices, as shown in [21, 68, 73, 96] for the 8-point case.

## 4 DCT Approximations with minimal angular error

In [68], a search space reduction based on the vector direction analysis [63, 45] of the transformation basis vectors was proposed. In the following, we summarize the method.

The exact DCT matrix  $\mathbf{C}_N$  can be understood as a stack of row vectors  $\mathbf{c}_k^\top$ ,  $k = 0, 1, \dots, N-1$ . The goal of the method is to find a low-complexity matrix  $\mathbf{T}_N$ , whose rows are denoted by  $\mathbf{t}_k^\top$ ,  $k = 0, 1, \dots, N-1$ , such that a prescribed error measure between the corresponding rows of the exact DCT and the approximation is minimized. The entries of  $\mathbf{t}_k^\top$  are selected from a set of  $\mathcal{D} = \{d_0, d_1, \dots, d_{D-1}\}$ , where  $d_i$ ,  $i = 0, 1, \dots, D-1$ , are low-complexity (trivial [8]) multipliers. Departing from the usual measures in the approximate transform literature, such as Euclidean distance, in [68], the angle between vectors is adopted as the error function. Thus, the following optimization problem is defined [68]:

$$\mathbf{t}_k = \underset{\mathbf{p} \in \mathcal{D}^N}{\text{argmin angle}(\mathbf{p}, \mathbf{c}_k)}, \quad k = 0, 1, \dots, N-1, \quad (5)$$

where  $\mathbf{p}^\top$  is a candidate row defined over the  $N$ -dimensional discrete space  $\mathcal{D}^N = \mathcal{D} \times \mathcal{D} \times \dots \times \mathcal{D}$ , the angle between two vectors,  $\mathbf{p}$  and  $\mathbf{c}_k$ , is given by

$$\text{angle}(\mathbf{p}, \mathbf{c}_k) = \arccos\left(\frac{\langle \mathbf{p}, \mathbf{c}_k \rangle}{\|\mathbf{p}\| \cdot \|\mathbf{c}_k\|}\right), \quad (6)$$

the symbol  $\langle \cdot, \cdot \rangle$  denotes the usual inner product, and  $\|\cdot\|$  is the norm induced by the inner product [92]. The resulting low-complexity matrix  $\mathbf{T}_N$  from the above optimization problem is said to have minimal angular

error relative to the exact DCT.

The search space implied by the above-described procedure contains  $D^N$  rows. Therefore, the computation described in (5) requires  $N \cdot D^N$  angle evaluations at most. In [68], it was adopted  $\mathcal{D} = \{-1, 0, 1\}$  ( $D = 3$ ) and  $N = 8$ , implying in only  $3^8 = 6561$  candidate rows. For larger values of  $N$ , the number of candidate rows are presented in Table 1, also considering  $\mathcal{D} = \{-1, 0, 1\}$ . Notice that any other discrete space with three elements will generate the same number of candidate rows. Hereafter the collection of all possible rows is called  $\mathcal{P}$ .

Table 1: The relation between matrix size and the number of candidate rows, considering a discrete space of three elements (e.g.  $\mathcal{D} = \{-1, 0, 1\}$ ).

$N$	Number of candidate rows
8	6561
16	43046721
32	$\approx 1.85 \times 10^{15}$
64	$\approx 3.43 \times 10^{30}$

The above procedure does not ensure the orthogonality of the resulting matrix. Although orthogonality is not strictly a necessary condition for the derivation of good DCT approximations (e.g., SDCT [38]), it is often a desirable design feature. To address such specific need, the optimization problem in (5) can be extended by the inclusion of an orthogonality constraint such that each new candidate row is compared against the previously obtained rows ensuring that their inner products are null [85]. However, the orthogonality constraint increases significantly the search time, since this restriction is sensitive to the order in which the rows are approximated, being feasible for small blocklengths only, as successfully demonstrated in [68] for  $N = 8$ . Algorithm 1 presents the pseudo-code that contains the unconstrained procedure.

---

**Algorithm 1** Pseudo-code for the unconstrained angle based method.

---

**Input:**  $\mathbf{C}_N, \mathcal{P}$

**Output:**  $\mathbf{T}_N$

---

```

1: for  $k \leftarrow 0, 1, \dots, N - 1$  do
2:    $\theta_{\min} \leftarrow 2\pi$ ;
3:   for  $i \leftarrow 0, 1, \dots, D^N - 1$  do
4:      $\mathbf{p} \leftarrow \mathcal{P}_i$ ;
5:      $\theta \leftarrow \text{angle}(\mathbf{p}, \mathbf{c}_k)$ ;
6:     if  $(\theta < \theta_{\min})$  then
7:        $\theta_{\min} \leftarrow \theta$ ;
8:        $\mathbf{t}_k \leftarrow \mathbf{p}$ ;
9:     end if
10:  end for
11:   $\mathbf{T}_N(k, :) \leftarrow \mathbf{t}_k$ ;
12: end for
13: return  $\mathbf{T}_N$ ;

```

---



and 64-point because of the computation time. The 16-, 32-, and 64-point low-complexity matrices obtained

Table 2: Total matrices and classes of equivalence obtained for the 16-, 32-, and 64-point DCT

Sets considered	$N$	Number of matrices obtained	Number of classes of equivalence
$\mathcal{D}_1, \mathcal{D}_2, \mathcal{D}_3, \mathcal{D}_4, \mathcal{D}_5, \mathcal{D}_6$	16	156	5
$\mathcal{D}_1, \mathcal{D}_2, \mathcal{D}_3$	32	3	2
$\mathcal{D}_1$	64	1	1

are denoted here as  $\mathbf{T}_{N,i}$ , where  $i$  and  $N$  refers to the equivalence class and the length of the low-complexity matrix, respectively. For the case  $N = 16$ , we have five new approximations obtained directly from the proposed method; for  $N = 32$ , two new matrices; and, considering  $N = 64$ , we have only one new matrix. The best performing matrices (as discussed in Section 5.3) are numerically shown in the Appendix.

Due to the size of the search space for some settings, we had to reduce the number of matrices according to the following procedure:

1. Split the exact DCT into two matrices as follows:

$$\mathbf{C}_N = \text{abs}(\mathbf{C}_N) \circ \text{sign}(\mathbf{C}_N),$$

where  $\text{abs}(\cdot)$  [4, pg. 10] returns the absolute value of its input,  $\text{sign}(\cdot)$  is the entry-wise signum function [14, pg. 286], and  $\circ$  represents the element wise multiplication [85, pg. 251];

2. Select  $\mathcal{D}$  and remove its negative elements, e.g.:  $\mathcal{D}_3^+ = \{0, 1, 2\}$ ;
3. Rewrite (5) replacing  $\mathbf{c}_k$  and  $\mathcal{D}$  with  $\text{abs}(\mathbf{c}_k)$  and  $\mathcal{D}^+$ , respectively, as follows:

$$\mathbf{t}_k^* = \underset{\mathbf{p} \in (\mathcal{D}^+)^N}{\text{argmin}} \text{angle}(\mathbf{p}, \text{abs}(\mathbf{c}_k)), \quad k = 0, 1, \dots, N-1; \quad (7)$$

4. Use (7) to approximate the rows of  $\text{abs}(\mathbf{C}_N)$  individually and obtain the low-complexity matrix  $\mathbf{T}_N^*$ ;
5. Obtain the low-complexity  $\mathbf{T}_N$  by:

$$\mathbf{T}_N = \mathbf{T}_N^* \circ \text{sign}(\mathbf{C}_N).$$

To further reduce the search space, the symmetries of  $\text{abs}(\mathbf{C}_N)$  were used. Notice that the  $j$ th and the  $(N-j-1)$ th column of  $\text{abs}(\mathbf{C}_N)$  are equals. Thus, we only need to find approximations for half of the values in each row. Using this property in (7), the computation requires  $N \cdot (D^+)^{\frac{N}{2}}$  angle evaluations at most. This search space reduction was only adopted for  $N = 32$  considering  $\mathcal{D}_2$  and  $\mathcal{D}_3$ ; and for  $N = 64$  considering  $\mathcal{D}_1$ .

## 5.2 JAM scaling method

In addition to the obtained matrices, we also derive scaled approximations according to the JAM scaling method described in [61]. A scaled approximation derived from the JAM method consists of an  $2N$ -point

transformation based on an  $N$ -point approximation related as follows:

$$\mathbf{T}_{2N} = \begin{bmatrix} \mathbf{P}_1 & \mathbf{P}_2 \end{bmatrix} \cdot \begin{bmatrix} \mathbf{T}_N & \\ & \mathbf{T}_N \end{bmatrix} \cdot \begin{bmatrix} \mathbf{I}_N & \bar{\mathbf{I}}_N \\ \bar{\mathbf{I}}_N & \mathbf{I}_N \end{bmatrix}, \quad (8)$$

where  $\mathbf{T}_N$  is an  $N$ -point approximation,  $\mathbf{I}_N$  and  $\bar{\mathbf{I}}_N$  are, respectively, the  $N$ -point identity and counter-identity matrices. Matrices  $\mathbf{P}_1$  and  $\mathbf{P}_2$  are permutations of  $2N \times N$  dimension. Matrix  $\mathbf{P}_1$  contains ones in positions  $(2i, i), i = 0, \dots, N-1$ , and zeros elsewhere; whereas  $\mathbf{P}_2$  presents ones in positions  $(2i+1, i), i = 0, \dots, N-1$ , and zeros elsewhere.

Thus, we scaled the low-complexity matrices that generate the best performing transforms for  $N=16$  and  $32$ , according to the assessment measurements displayed in Table 3, through the JAM method. The scaling method is a function  $f$  defined according to:

$$\begin{aligned} f: \mathbb{R}^{N \times N} &\longrightarrow \mathbb{R}^{2N \times 2N} \\ \mathbf{T}_N &\longrightarrow \mathbf{T}_{2N} = f(\mathbf{T}_N). \end{aligned}$$

We denote  $\mathbf{T}_N^{(j)}$  as the  $2^j \cdot N \times 2^j \cdot N$  matrix based on  $\mathbf{T}_N$ :

$$\mathbf{T}_N^{(j)} \triangleq f(f(\dots f(\mathbf{T}_N))),$$

where function  $f$  is applied  $j$  times.

The proposed method in [61] has a term of  $\frac{1}{\sqrt{2}}$  that multiplies (8) which was previously omitted in the scaling to be integrated in the final quantization. Thus, the approximation  $\hat{\mathbf{C}}_N^{(j)}$  is obtained by

$$\hat{\mathbf{C}}_N^{(j)} = \left( \frac{1}{\sqrt{2}} \right)^j \cdot \mathbf{S}_N^* \cdot \mathbf{T}_N^{(j)}, \quad (9)$$

where  $\mathbf{S}_N^*$  is computed from  $\mathbf{T}_N^{(j)}$  as detailed in (4), *mutatis mutandis*. For instance,  $\hat{\mathbf{C}}_{16}^{(2)}$  is the result of two JAM applications in a 16-point matrix, resulting in a 64-point matrix.

### 5.3 Performance assessment

We evaluated the proposed approximations according to similarity measures and coding measures. For similarity measures, we considered the mean square error (MSE) [14, 67] and the total energy error ( $\epsilon$ ) [20]; whereas for coding measures, we adopted the unified coding gain ( $C_g$ ) [48] and the transform efficiency ( $\eta$ ) [14]. Based on the deviation from diagonality [33], we can also quantify the deviation from orthogonality ( $\delta(\cdot)$ ) of the discussed approximations; this measure informs how close to orthogonality a matrix is and is given by:

$$\delta(\mathbf{A}) = 1 - \frac{\|\text{diag}(\mathbf{A})\|_F}{\|\mathbf{A}\|_F}, \quad (10)$$

where  $\mathbf{A}$  is a square matrix and  $\|\cdot\|_F$  is the Frobenius norm for matrices [85].

For comparison purposes, we considered a comprehensive set of approximations archived in literature. For  $N=16$ , the following approximations were separated: (i) the approximation proposed by

Haweel ( $\widehat{\mathbf{C}}_{16,\text{SDCT}}$ ) [38] (ii) the approximation proposed by Jridi, Alfalou, and Meher ( $\widehat{\mathbf{C}}_{16,\text{JAM}}$ ) [61]; (iii) the approximation proposed by Bouguezel, Ahmad, and Swamy, ( $\widehat{\mathbf{C}}_{16,\text{BAS}}$ ), in [13]; (iv) the approximation proposed in [6], ( $\widehat{\mathbf{C}}_{16,\text{BCEM}}$ ); (v) the approximation introduced in [27], ( $\widehat{\mathbf{C}}_{16,\text{SOBCM}}$ ), and (vi) the scaled approximation proposed in [68] ( $T_{(16)}$ ), ( $\widehat{\mathbf{C}}_{16,\text{OCBSML}}$ ).

For  $N = 32$ , we considered the following methods: (i) the approximation proposed by Haweel ( $\widehat{\mathbf{C}}_{32,\text{SDCT}}$ ) [38]; (ii) the approximation proposed by Jridi, Alfalou, and Meher ( $\widehat{\mathbf{C}}_{32,\text{JAM}}$ ) [61]; (iii) the approximation proposed by Bouguezel, Ahmad, and Swamy, ( $\widehat{\mathbf{C}}_{32,\text{BAS}}$ ), in [13]; (vi) the scaled approximation proposed in [68] ( $T_{(32)}$ ), ( $\widehat{\mathbf{C}}_{32,\text{OCBSML}}$ ).

For  $N = 64$ , we considered the following approximations: (i) the approximation proposed by Haweel ( $\widehat{\mathbf{C}}_{64,\text{SDCT}}$ ) [38]; (ii) the scaled version of the approximation proposed in [68], ( $\widehat{\mathbf{C}}_{64,\text{OCBSML}}$ ).

Table 3 displays the results for the performance measures of the proposed approximations along with the competing approximations and the exact  $N$ -point DCT ( $\mathbf{C}_N$ ). For each value of  $N$ , we highlighted the best measurements of each metric. We identify  $\widehat{\mathbf{C}}_{16,5}$ ,  $\widehat{\mathbf{C}}_{32,2}$ ,  $\widehat{\mathbf{C}}_{16,5}^{(1)}$ ,  $\widehat{\mathbf{C}}_{64,1}$ , and  $\widehat{\mathbf{C}}_{16,5}^{(2)}$  as the best transforms for  $N = 16, 32$ , and  $64$ , respectively. Approximations  $\widehat{\mathbf{C}}_{16,5}$ ,  $\widehat{\mathbf{C}}_{32,2}$ , and  $\widehat{\mathbf{C}}_{64,1}$  are the low-complexity matrices obtained from the fifth, second, and first class of equivalence for  $N = 16, 32$ , and  $64$ , respectively. The approximations  $\widehat{\mathbf{C}}_{16,5}^{(1)}$  and  $\widehat{\mathbf{C}}_{16,5}^{(2)}$  are the scaled approximations based on  $\widehat{\mathbf{C}}_{16,5}$ . These proposed approximations outperformed the DCT approximations already known in the literature.

## 5.4 Fast algorithms

In order to reduce the arithmetic cost we factorized the best transforms into sparse matrices considering usual decimation-based techniques [8, pg. 74]. The factorization for the proposed transforms was developed using butterfly-based structures, such as in [40, 107, 79, 20, 21]. The complexity of the fast algorithms was evaluated in terms of the number of arithmetic operations. The arithmetic complexity does not depend on the available technology, an issue that occurs in measures such as computation time [69, 52]. Table 4 presents the arithmetic complexity of the proposed transforms before and after the matrix factorization and also the percentage of complexity reduction.

Although the matrices  $\mathbf{T}_{16,\text{OCBSML}}$ ,  $\mathbf{T}_{32,\text{OCBSML}}$ , and  $\mathbf{T}_{64,\text{OCBSML}}$  [68] are more benefited by factorization, with a few more operations, the proposed approximations can be used, providing better performance. According to Table 3 and 4, when comparing  $\mathbf{T}_{16,\text{OCBSML}}$  and  $\mathbf{T}_{16,5}$ , the proposed approximation requires only 16 more additions but it presents a reduction of approximately 96% and 93% in terms of energy error and MSE, respectively; and a gain of approximately 2.8% in coding gain and 4.7% in transform efficiency.

Considering  $N = 32$ , the proposed approximation  $\mathbf{T}_{32,1}$  needs 127 extra additions than  $\mathbf{T}_{32,\text{OCBSML}}$  and it presents a reduction of approximately 95% and 93% of energy error and MSE, respectively; and a improvement of 1.6% in coding gain and 6.4% in transform efficiency. In addition, the proposed approximation  $\mathbf{T}_{16,5}^{(1)}$  requires 72 more additions than  $\mathbf{T}_{32,\text{OCBSML}}$  and it presents a reduction of 54% and 33% of energy error and MSE, respectively; and a gain of approximately 2.7% in coding gain and 6.5% in transform efficiency. Approximations for  $N = 64$  (except the SDCT) were first presented in this paper.

For better understanding and reproducibility, each sparse matrix used to obtain low-complexity matrices associated with the optimal transforms  $\mathbf{T}_{16,5}$ ,  $\mathbf{T}_{32,2}$ , and  $\mathbf{T}_{64,1}$  are detailed in Appendix.

Table 3: Performance measures for the DCT approximations in literature and the new approximations proposed

Approximation	$\epsilon(\hat{\mathbf{C}})$	MSE( $\hat{\mathbf{C}}$ )	$C_g(\hat{\mathbf{C}})$	$\eta(\hat{\mathbf{C}})$	$\delta(\hat{\mathbf{C}})$
$N = 16$					
$\mathbf{C}_{16}$	0	0	9.4555	88.4518	0
$\hat{\mathbf{C}}_{16,1}$	3.7043	0.0172	7.7474	70.5034	0.0828
$\hat{\mathbf{C}}_{16,2}$	3.7043	0.0172	8.2190	70.6902	0.0270
$\hat{\mathbf{C}}_{16,3}$	1.0227	0.0054	8.9653	78.4016	0.0472
$\hat{\mathbf{C}}_{16,4}$	0.6337	0.0035	9.0922	80.1145	0.0234
$\hat{\mathbf{C}}_{16,5}$	<b>0.5748</b>	<b>0.0031</b>	<b>9.1268</b>	<b>80.4401</b>	0.0118
$\hat{\mathbf{C}}_{16,\text{SDCT}}$	8.2537	0.0429	6.0297	64.9653	0.2
$\hat{\mathbf{C}}_{16,\text{JAM}}$	14.7402	0.0506	8.4285	72.2296	0
$\hat{\mathbf{C}}_{16,\text{BAS}}$	16.4071	0.0564	8.5208	73.6345	0
$\hat{\mathbf{C}}_{16,\text{BCEM}}$	8.0806	0.0465	7.8401	65.2789	0
$\hat{\mathbf{C}}_{16,\text{SOBCM}}$	40.9996	0.0947	7.8573	67.6078	0
$\hat{\mathbf{C}}_{16,\text{OCBSML}}$	13.7032	0.0474	8.8787	76.8108	0
$N = 32$					
$\mathbf{C}_{32}$	0	0	9.7736	81.6962	0
$\hat{\mathbf{C}}_{32,1}$	7.6403	0.0287	7.4624	52.5455	0.1138
$\hat{\mathbf{C}}_{32,2}$	<b>2.3525</b>	<b>0.0100</b>	9.0983	64.9265	0.0376
$\hat{\mathbf{C}}_{16,5}^{(1)}$	30.0539	0.0829	<b>9.1939</b>	<b>64.9983</b>	0.0118
$\hat{\mathbf{C}}_{32,\text{SDCT}}$	18.2386	0.0748	5.5623	41.6653	0.2727
$\hat{\mathbf{C}}_{32,\text{JAM}}$	48.0956	0.1124	8.5010	56.9700	0
$\hat{\mathbf{C}}_{32,\text{BAS}}$	57.1260	0.1171	8.4971	58.1727	0
$\hat{\mathbf{C}}_{32,\text{OCBSML}}$	46.2658	0.1104	8.9505	61.0272	0
$N = 64$					
$\mathbf{C}_{64}$	0	0	9.9366	75.55406	0
$\hat{\mathbf{C}}_{64,1}$	<b>15.5707</b>	<b>0.0434</b>	7.2436	36.4275	0.1152
$\hat{\mathbf{C}}_{16,5}^{(2)}$	103.2435	0.1833	<b>9.2144</b>	<b>51.6925</b>	0.0118
$\hat{\mathbf{C}}_{32,2}^{(1)}$	66.8310	0.1355	9.1164	51.2582	0.0376
$\hat{\mathbf{C}}_{64,\text{SDCT}}$	38.2630	0.1141	5.2192	27.9725	0.2809
$\hat{\mathbf{C}}_{64,\text{OCBSML}}$	125.2247	0.2015	8.9748	48.4443	0

## 6 Image compression experiments

To evaluate the performance of the proposed 16-, 32-, and 64-point DCT approximations we performed JPEG-like image compression experiments, as in [20, 21, 72]. We considered 45 8-bit images of  $512 \times 512$  obtained from [99]. All images were subdivided into  $N \times N$  sub-blocks and were submitted to the following 2D transformation. Let  $\mathbf{A}$  be an  $N \times N$  sub-block. The direct and inverse transformation induced by  $\hat{\mathbf{C}}_N$  are given, respectively, by [95, 21, 20]:

$$\mathbf{B} = \hat{\mathbf{C}}_N \cdot \mathbf{A} \cdot \hat{\mathbf{C}}_N^{-1} \quad \text{and} \quad \mathbf{A} = \hat{\mathbf{C}}_N^{-1} \cdot \mathbf{B} \cdot \hat{\mathbf{C}}_N, \quad (11)$$

Table 4: The arithmetic complexity of the proposed transforms before and after the matrix factorization.

Matrix	Before factorization			After factorization		Reduction (%)	
	Mult	Adds	Bit-shifting	Adds	Bit-shifting	Adds	Bit-shifting
$N = 16$							
$\mathbf{C}_{16}$	256	240	0	-	-	-	-
$\mathbf{T}_{16,1}$	0	184	0	82	0	55.44	0
$\mathbf{T}_{16,2}$	0	192	0	80	0	58.33	0
$\mathbf{T}_{16,3}$	0	208	80	88	30	57.69	62.50
$\mathbf{T}_{16,4}$	0	224	96	92	34	58.93	73.44
$\mathbf{T}_{16,5}$	0	240	160	100	62	58.33	64.77
$\mathbf{T}_{16,OCBSML}$	0	208	96	64	12	69.23	79.17
$N = 32$							
$\mathbf{C}_{32}$	1024	992	0	-	-	-	-
$\mathbf{T}_{32,1}$	0	752	0	287	0	61.83	0
$\mathbf{T}_{32,2}$	0	864	320	328	110	62.04	65.62
$\mathbf{T}_{16,5}^{(1)}$	0	992	640	232	124	76.61	80.62
$\mathbf{T}_{32,OCBSML}$	0	864	384	160	24	81.48	89.58
$N = 64$							
$\mathbf{C}_{64}$	4096	4032	0	-	-	-	-
$\mathbf{T}_{64,1}$	0	3040	0	1087	0	64.24	0
$\mathbf{T}_{16,5}^{(2)}$	0	4032	2560	528	248	86.90	90.31
$\mathbf{T}_{32,2}^{(1)}$	0	3520	1280	720	220	79.54	82.81
$\mathbf{T}_{64,OCBSML}$	0	3520	1536	384	48	89.09	94.79

where  $\mathbf{A}$  and  $\mathbf{B}$  are matrices of size  $N \times N$ . To evaluate the exact DCT, the transformation matrix  $\widehat{\mathbf{C}}_N$  and  $\widehat{\mathbf{C}}_N^{-1}$  are replaced by  $\mathbf{C}_N$  and  $\mathbf{C}_N^{-1}$ , respectively. Considering the zig-zag pattern [82, pg. 30], we retained the initial  $r$  coefficients from each sub-block  $\mathbf{B}$ . Finally, we applied the inverse 2D transform in each sub-block, and then the compression images are obtained.

Original and compressed images were evaluated considering usual quality assessment measures: (i) the mean square error (MSE) [14], (ii) the peak signal-to-noise ratio (PSNR) [82], and (iii) the mean structural similarity index (MSSIM) [105]. Notice that the MSE measures are computed considering the original and the compressed images; not to be confused with the MSE calculation described in Section 5.3. Although the MSE and PSNR measures are popular in the context of image compression, it was shown in [104] that they might offer limited results as image quality tools. On the other hand, the MSSIM was shown to be a better measure when it comes to capturing the image quality as understood by the human visual system model [105, 104].

The image compression experiments were divided into two steps: (i) a qualitative analysis where we considered the compressed *Peppers* image with a compression rate of approximately 80%; (ii) and a quantitative analysis, where we considered the average measurements from 45 standardized images. Both analysis are presented next.

## 6.1 Qualitative analysis

For the qualitative analysis, we considered the compressed *Peppers* image [99], with a compression rate (CR) of approximately 80%. The compression rate is defined by:

$$\text{CR} = 1 - \frac{r}{N^2}.$$

Fig. 1, 2, and 3 display the compressed *Peppers* images with the DCT and approximations, for  $N = 16, 32,$  and  $64,$  respectively. Visually, the reconstructed images after the compression with the proposed transforms exhibit quality comparable to the ones compressed using the exact DCT and known approximations. For a better representation, we present the MSE, PSNR, and MSSIM of these images in Table 5. The best results for each sample image and measure are highlighted. **The proposed approximations for the 16-, 32-, and 64-point DCT show better results than the approximations in literature.** To the best of our knowledge, there is no 64-point DCT approximation in the literature for comparison, except for the  $\hat{C}_{64,SDCT}$  [38].

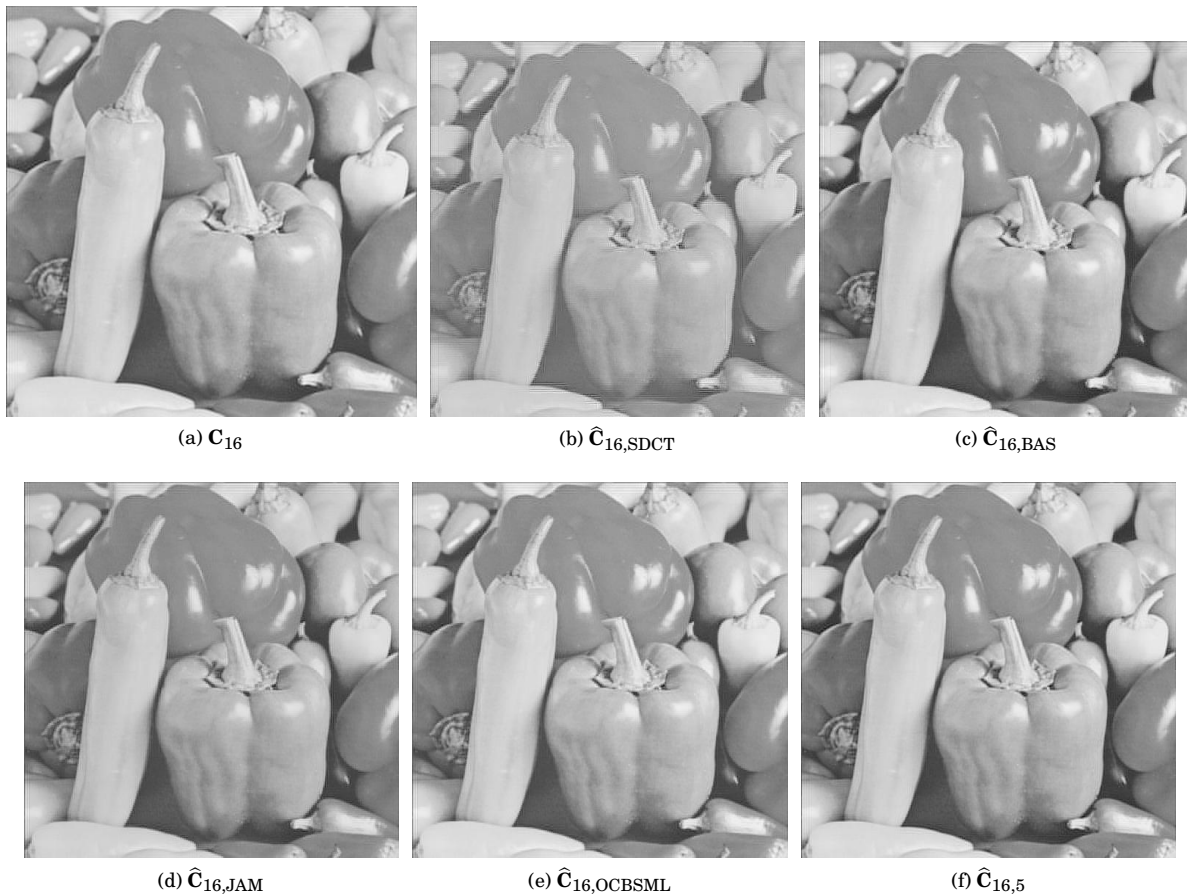


Figure 1: Compressed *Peppers* image for  $N = 16$  considering  $r = 50$ .

## 6.2 Quantitative analysis

In this analysis, we considered the measurements of the selected 45 8-bit images obtained from a public image bank [99]. Each image was compressed considering the initial  $r$  coefficient (matrix elements ordered according to the zig-zag pattern),  $r \in \{0, 1, \dots, N^2\}$ , and assessed by the quality measures.

Fig. 4, 5, and 6 show the average curves from the 45 images for the MSE, PSNR, and MSSIM, respectively.

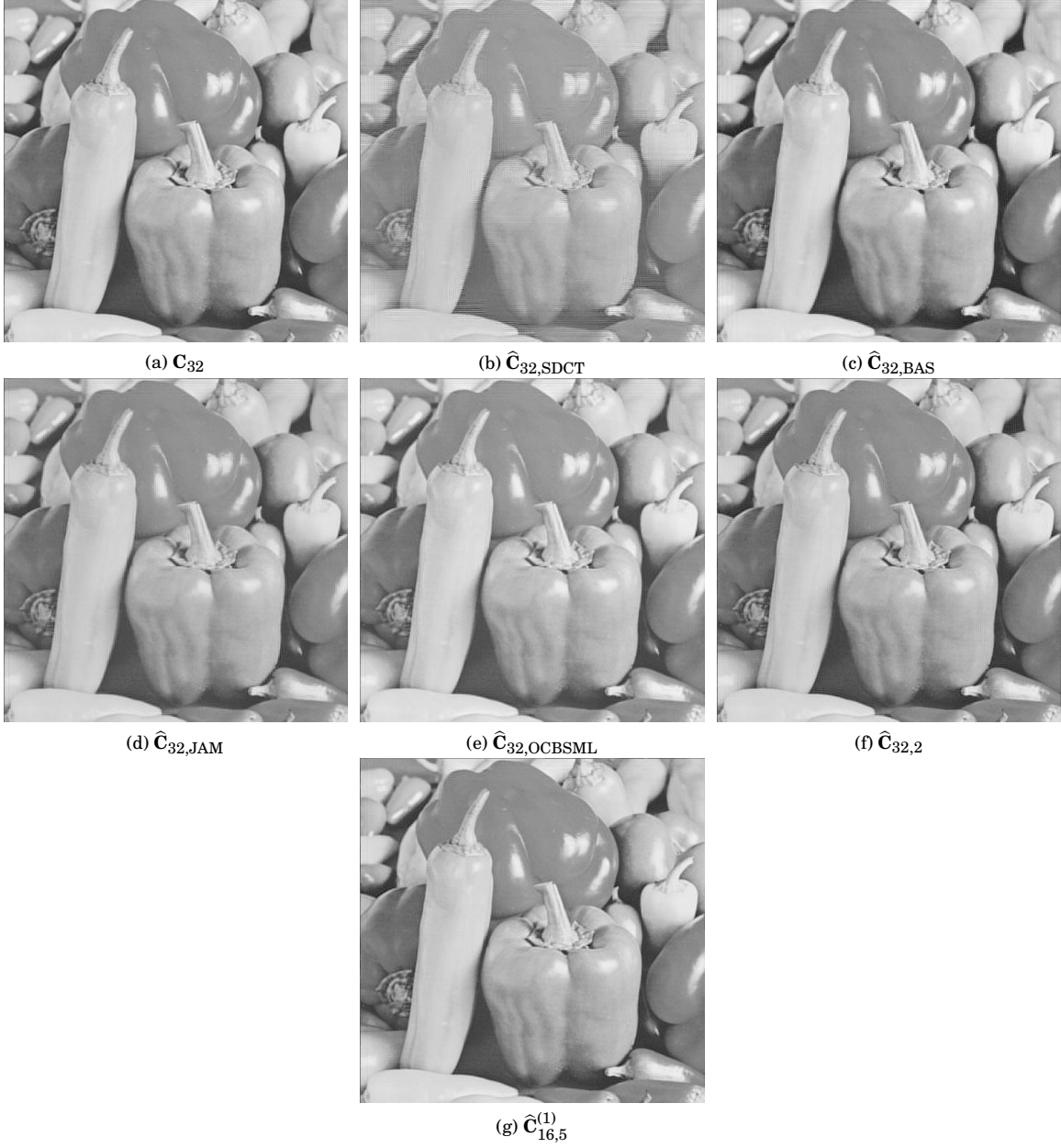


Figure 2: Compressed *Peppers* image for  $N = 32$  considering  $r = 205$ .

For better visualization, we adopted the absolute percentage error (APE) relative to the DCT:

$$\text{APE}(\mu) = \left| \frac{\mu(\mathbf{C}_N) - \mu(\hat{\mathbf{C}}_N)}{\mu(\mathbf{C}_N)} \right|, \quad \mu \in \{\text{MSE}, \text{PSNR}, \text{MSSIM}\},$$

where  $\mu(\mathbf{C}_N)$  and  $\mu(\hat{\mathbf{C}}_N)$  indicate the measurements according to the exact and approximate  $N$ -point DCT, respectively. For this evaluation, we considered the optimal proposed transforms  $\hat{\mathbf{C}}_{16,5}$ ,  $\hat{\mathbf{C}}_{32,2}$ ,  $\hat{\mathbf{C}}_{16,5}^{(1)}$ ,  $\hat{\mathbf{C}}_{64,1}$ ,  $\hat{\mathbf{C}}_{16,5}^{(2)}$ , and  $\hat{\mathbf{C}}_{32,2}^{(1)}$  and compared with the exact DCT ( $\mathbf{C}_N$ ) and the three best approximations according to

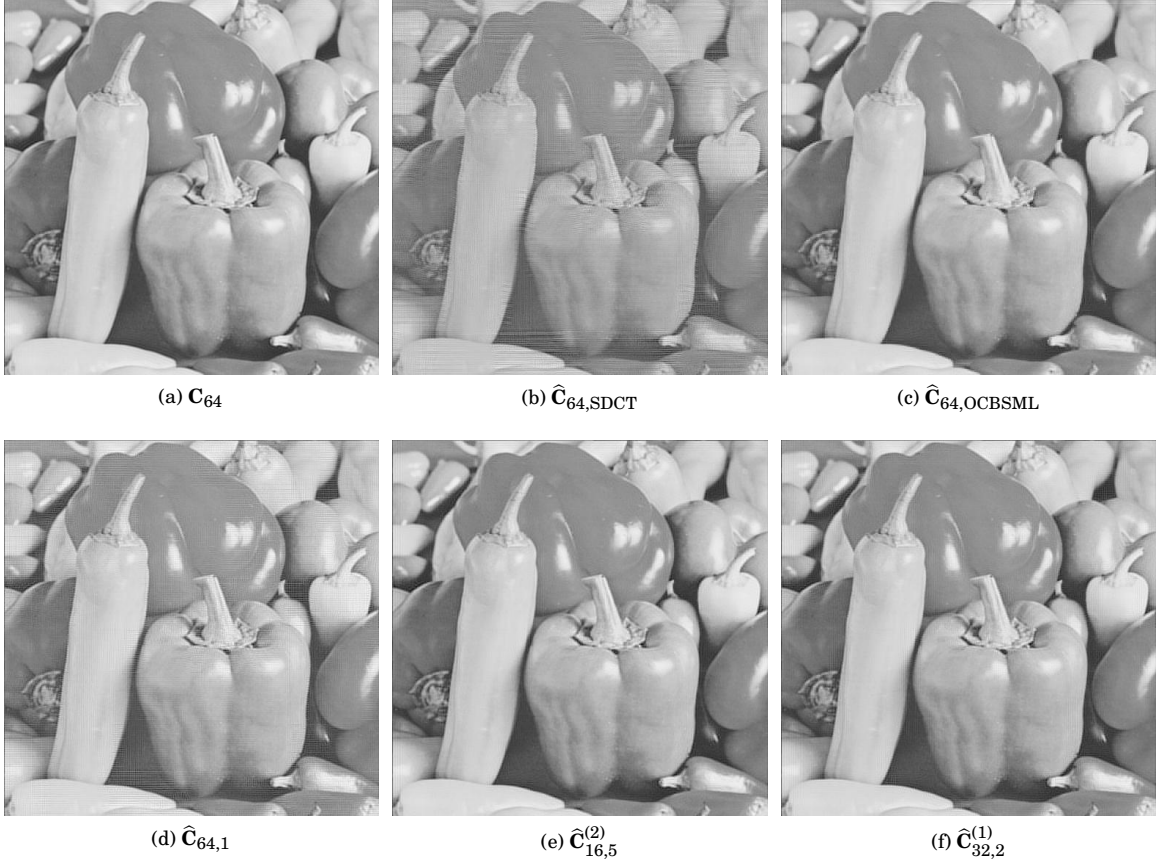


Figure 3: Compressed *Peppers* image for  $N = 64$  considering  $r = 820$ .

Table 3:  $\hat{\mathbf{C}}_{N,\text{BAS}}$ ,  $\hat{\mathbf{C}}_{N,\text{JAM}}$ , and  $\hat{\mathbf{C}}_{N,\text{OCBSML}}$ . **The proposed approximations are the ones with the best results when contrasted with competing DCT approximations for  $N = 16, 32,$  and  $64$ .**

Table 5: Image quality measures of compressed *Peppers* image for  $N = 16(r = 50)$ ,  $32(r = 205)$ , and  $64(r = 820)$ .

$N$	Approximation	MSE	PSNR	MSSIM
16	$\mathbf{C}_{16}$	<b>32.3449</b>	<b>33.0328</b>	<b>0.9416</b>
	$\tilde{\mathbf{C}}_{16,1}$	75.0342	29.3782	0.9154
	$\tilde{\mathbf{C}}_{16,2}$	70.1802	29.6687	0.9184
	$\tilde{\mathbf{C}}_{16,3}$	43.2034	31.7756	0.9355
	$\tilde{\mathbf{C}}_{16,4}$	39.0721	32.2121	<b>0.9378</b>
	$\tilde{\mathbf{C}}_{16,5}$	<b>38.8975</b>	<b>32.2316</b>	<b>0.9378</b>
	$\tilde{\mathbf{C}}_{16,\text{SDCT}}$	135.8288	26.8009	0.8905
	$\tilde{\mathbf{C}}_{16,\text{JAM}}$	59.6891	30.3718	0.9242
	$\tilde{\mathbf{C}}_{16,\text{BAS}}$	58.1761	30.4834	0.9248
	$\tilde{\mathbf{C}}_{16,\text{BCEM}}$	93.1786	28.4376	0.9064
	$\tilde{\mathbf{C}}_{16,\text{SOBCM}}$	115.2820	27.5132	0.8897
	$\tilde{\mathbf{C}}_{16,\text{OCBSML}}$	49.3669	31.1964	0.9303
	32	$\mathbf{C}_{32}$	<b>29.2562</b>	<b>33.4686</b>
$\tilde{\mathbf{C}}_{32,1}$		87.8409	28.6938	0.9443
$\tilde{\mathbf{C}}_{32,2}$		43.5848	31.7375	0.9634
$\tilde{\mathbf{C}}_{16,5}^{(1)}$		<b>37.8366</b>	<b>32.3517</b>	<b>0.9652</b>
$\tilde{\mathbf{C}}_{32,\text{SDCT}}$		189.2796	25.3598	0.9122
$\tilde{\mathbf{C}}_{32,\text{JAM}}$		58.4496	30.4630	0.9554
$\tilde{\mathbf{C}}_{32,\text{BAS}}$		61.6647	30.2304	0.9524
$\tilde{\mathbf{C}}_{32,\text{OCBSML}}$		47.9872	31.3196	0.9591
64	$\mathbf{C}_{64}$	<b>28.1330</b>	<b>33.6386</b>	<b>0.9880</b>
	$\tilde{\mathbf{C}}_{64,1}$	118.8871	27.3795	0.9641
	$\tilde{\mathbf{C}}_{16,5}^{(2)}$	<b>37.3748</b>	<b>32.4050</b>	<b>0.9851</b>
	$\tilde{\mathbf{C}}_{32,2}^{(1)}$	42.8390	31.8124	0.9836
	$\tilde{\mathbf{C}}_{64,\text{SDCT}}$	273.3575	23.7635	0.9294
	$\tilde{\mathbf{C}}_{64,\text{OCBSML}}$	54.2638	30.7857	0.9794

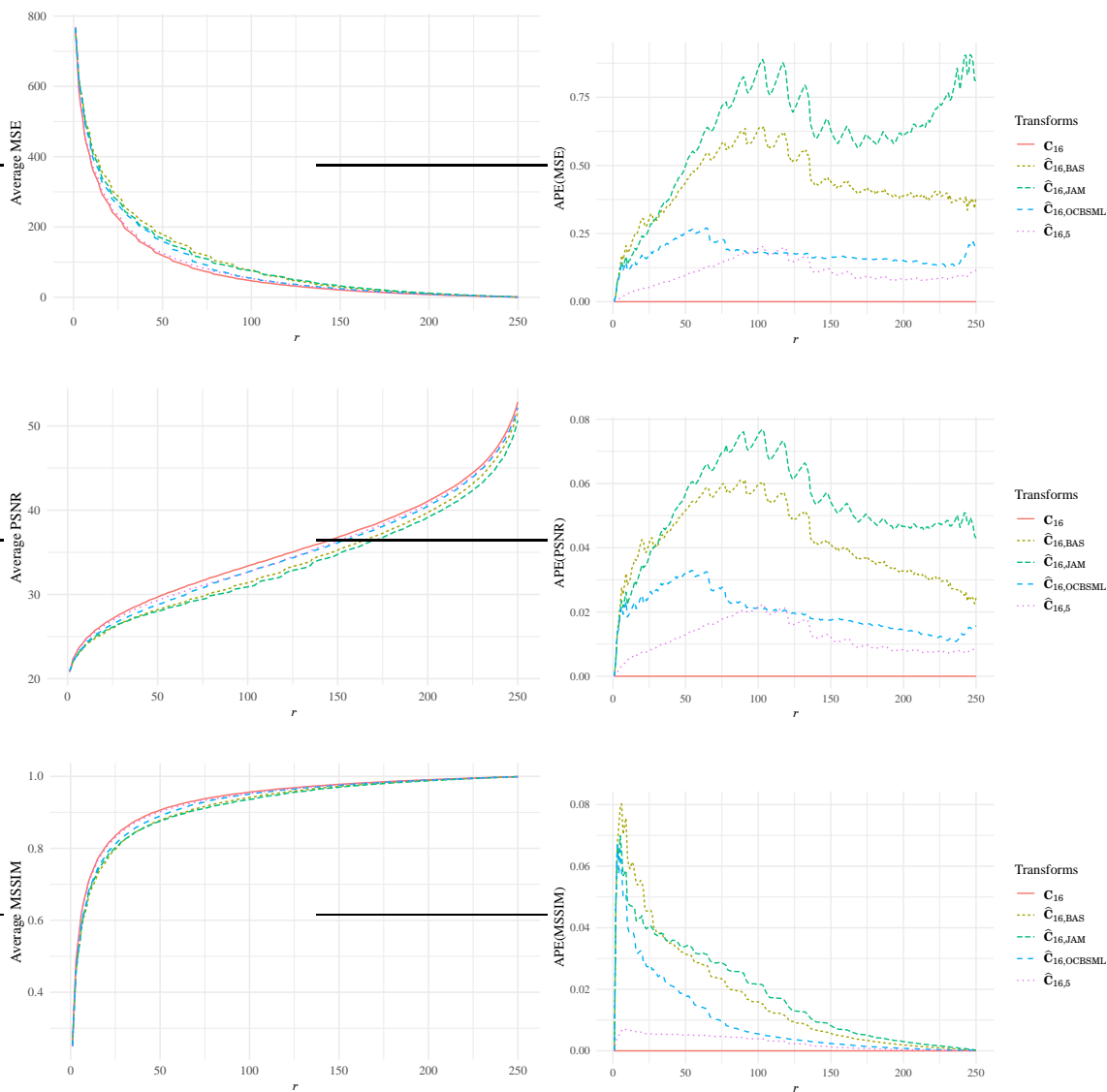


Figure 4: Average curves for the MSE, PSNR, and MSSIM for the 16-point DCT and approximations.

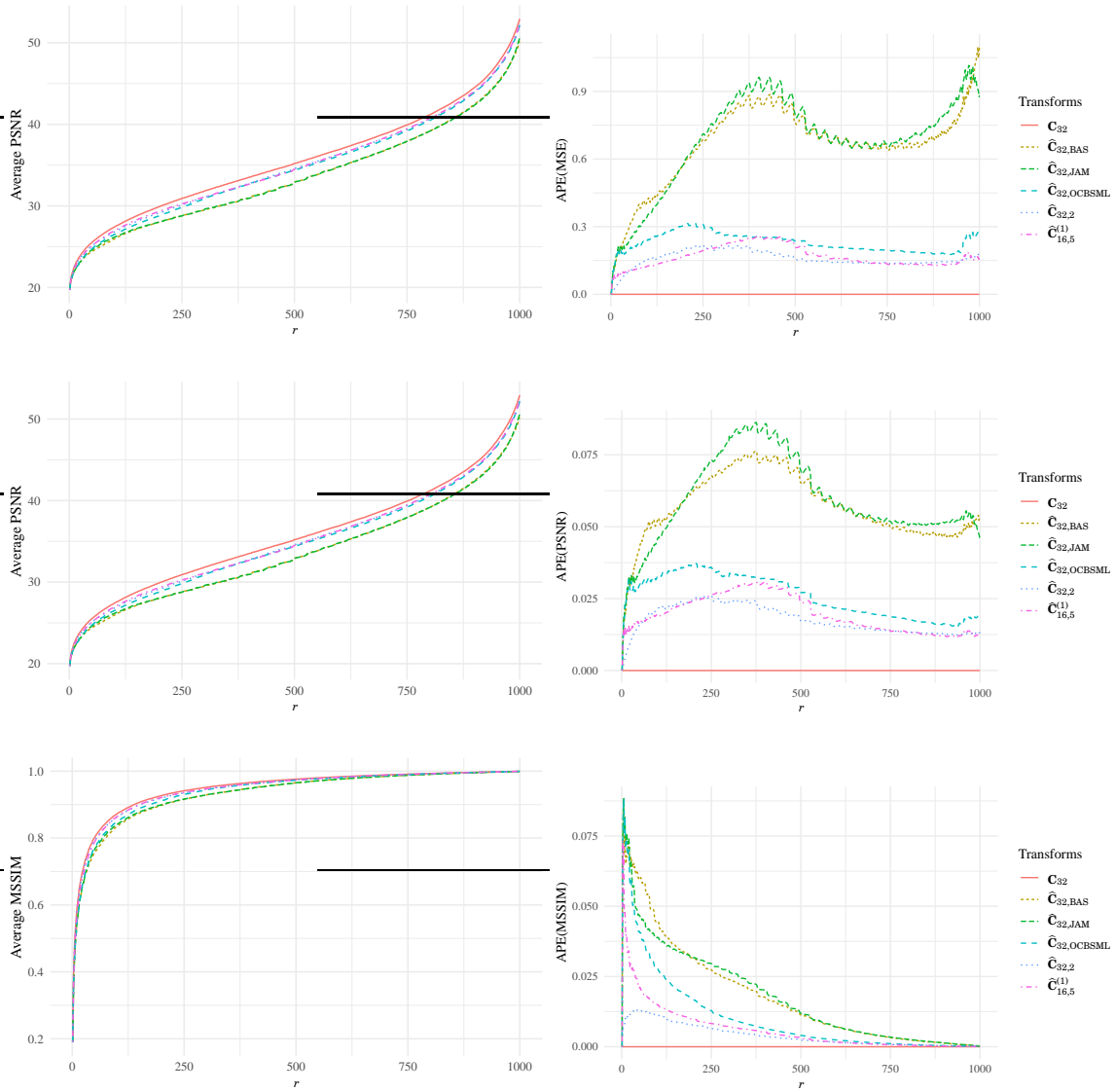


Figure 5: Average curves for the MSE, PSNR, and MSSIM for the 32-point DCT and approximations.

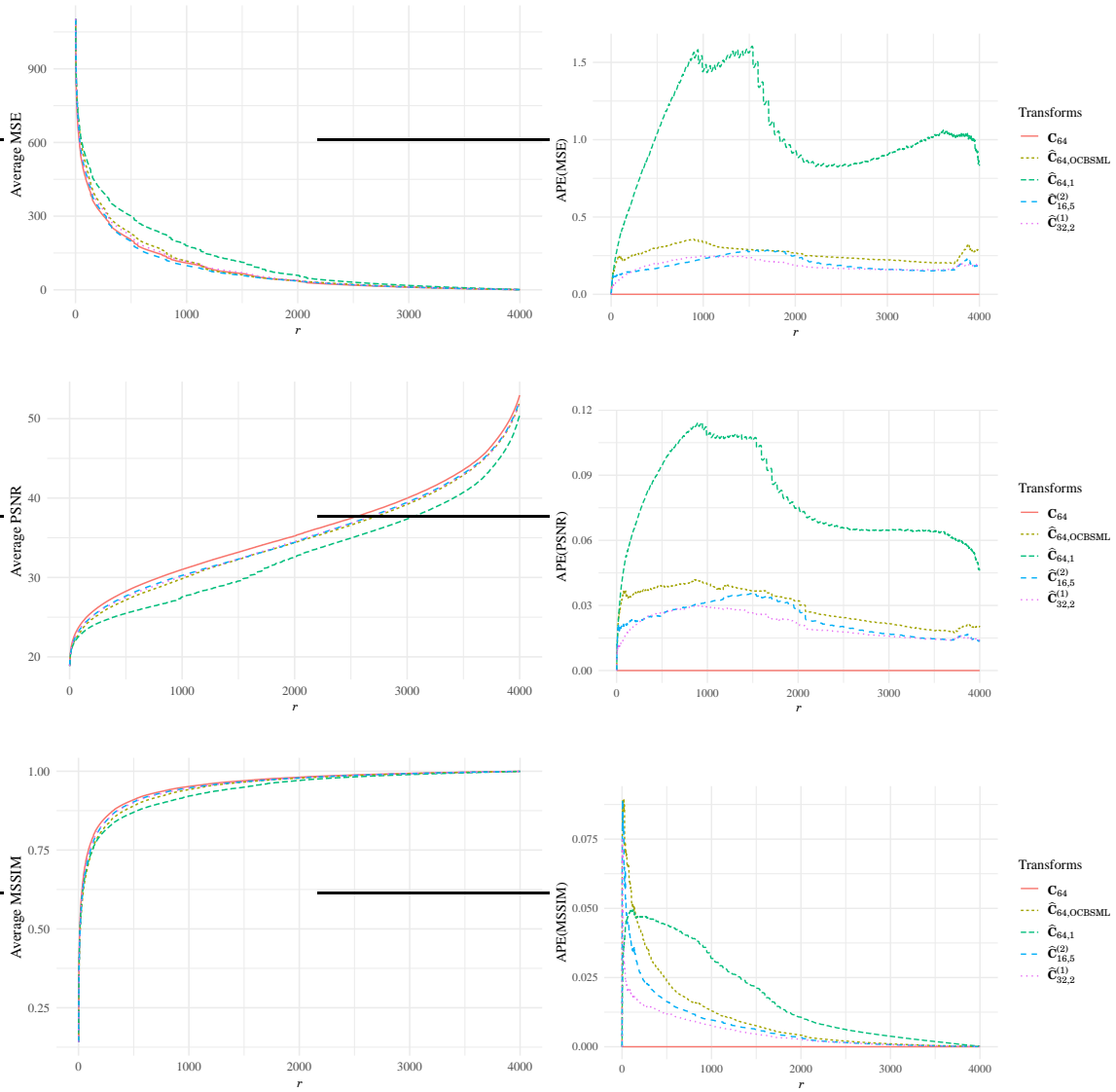


Figure 6: Average curves for the MSE, PSNR, and MSSIM for the 64-point DCT and approximations.

## 7 Conclusions

This paper introduces low-complexity approximations for the DCT of lengths 16, 32, and 64, based on the method proposed in [68], which approximates the rows of the exact and the approximate matrix transform according to the angle between them. The proposed transforms were assessed according to classical figures of merit and showed an outstanding performance when compared to the DCT approximations already archived in the literature. Fast algorithms were also derived for the best transforms of each blocklength, which further reduced their arithmetic costs. Only additions and bit-shifting operations are necessary for their computation. Besides, the transforms were evaluated in the context of image compression. *The experiments demonstrated that the proposed transforms outperformed all the considered DCT approximations already known in the literature for  $N = 16, 32, \text{ and } 64$ .*

## Acknowledgments

We gratefully acknowledge partial financial support from *Coordenação de Aperfeiçoamento de Pessoal de Nível Superior (CAPES)*, *Conselho Nacional de Desenvolvimento Científico e Tecnológico (CNPq)*, and *Fundação de Amparo a Ciência e Tecnologia de Pernambuco (FACEPE)*, Brazil.

## A Matrix Factorization

The matrices used in the Section 5.4 are detailed here. First, consider the following butterfly-structure:

$$\mathbf{B}_N = \begin{bmatrix} \mathbf{I}_{\frac{N}{2}} & \bar{\mathbf{I}}_{\frac{N}{2}} \\ -\bar{\mathbf{I}}_{\frac{N}{2}} & \mathbf{I}_{\frac{N}{2}} \end{bmatrix}.$$

For the sake of brevity, cycle notation [30, 108, 81] is used to present the permutation matrices. The resulting permutation matrix is obtained by permuting the columns of the identity matrix following the cycle mapping zero indexed.

### A.1 Matrix Factorization for $N = 16$

The low-complexity matrix  $\mathbf{T}_{16,5}$  can be represented as:

$$\mathbf{T}_{16,5} = \mathbf{P}_{16} \cdot \mathbf{M}_{16} \cdot \begin{bmatrix} \mathbf{B}_2 & \\ & \mathbf{I}_{14} \end{bmatrix} \cdot \begin{bmatrix} \mathbf{B}_4 & \\ & \mathbf{I}_{12} \end{bmatrix} \cdot \begin{bmatrix} \mathbf{B}_8 & \\ & \mathbf{I}_8 \end{bmatrix} \cdot \mathbf{B}_{16}$$

where

$$\mathbf{P}_{16} = (1\ 8)(2\ 4)(3\ 12\ 9)(5\ 6\ 10)(7\ 14\ 13\ 11),$$







## References

- [1] N. AHMED, T. NATARAJAN, AND K. R. RAO, *Discrete cosine transform*, IEEE Transactions on Computers, C-23 (1974), p. 90–93.
- [2] H. A. ALMURIB, T. N. KUMAR, AND F. LOMBARDI, *Approximate DCT image compression using inexact computing*, IEEE Transactions on Computers, 67 (2018), p. 149–159.
- [3] A. N. BAHAR AND K. A. WAHID, *Design and implementation of approximate DCT architecture in quantum-dot cellular automata*, IEEE Transactions on Very Large Scale Integration (VLSI) Systems, 28 (2020), p. 2530–2539.
- [4] R. G. BARTLE AND D. R. SHERBERT, *Introduction to real analysis*, vol. 2, Wiley New York, 2000.
- [5] F. M. BAYER AND R. J. CINTRA, *DCT-like transform for image compression requires 14 additions only*, Electronics Letters, 48 (2012), p. 919–921.
- [6] F. M. BAYER, R. J. CINTRA, A. EDIRISURIYA, AND A. MADANAYAKE, *A digital hardware fast algorithm and FPGA-based prototype for a novel 16-point approximate DCT for image compression applications*, Measurement Science and Technology, 23 (2012).
- [7] E. BELYAEV, L. BIE, AND J. KORHONEN, *Motion JPEG decoding via iterative thresholding and motion-compensated deflickering*, in 2020 IEEE 22nd International Workshop on Multimedia Signal Processing (MMSP), 2020, p. 1–6.
- [8] R. E. BLAHUT, *Fast algorithms for signal processing*, Cambridge University Press, 2nd ed., 2010.
- [9] S. BOUGUEZEL, M. O. AHMAD, AND M. SWAMY, *A multiplication-free transform for image compression*, in 2008 2nd International Conference on Signals, Circuits and Systems, 2008, p. 1–4.
- [10] ———, *A low-complexity parametric transform for image compression*, in 2011 IEEE International Symposium of Circuits and Systems, 2011, p. 2145–2148.
- [11] S. BOUGUEZEL, M. O. AHMAD, AND M. N. S. SWAMY, *Low-complexity  $8 \times 8$  transform for image compression*, Electronics Letters, 44 (2008), p. 1249–1250.
- [12] ———, *A fast  $8 \times 8$  transform for image compression*, in International Conference on Microelectronics, Dec. 2009, p. 74–77.
- [13] ———, *A novel transform for image compression*, in 2010 53rd IEEE International Midwest Symposium on Circuits and Systems, Aug. 2010, p. 509–512.
- [14] V. BRITANAK, P. YIP, AND K. R. RAO, *Discrete Cosine and Sine Transforms*, Academic Press, 2007.
- [15] A. J. BUSSON, P. R. MENDES, D. S. DE MORAES, ÁLVARO M. DA VEIGA, ÁLAN L. V. GUEDES, AND S. COLCHER, *Video quality enhancement using deep learning-based prediction models for quantized DCT coefficients in MPEG I-frames*, in 2020 IEEE International Symposium on Multimedia (ISM), 2020, p. 29–32.
- [16] G. CAMPOBELLO, A. SEGRETO, S. ZANAFI, AND S. SERRANO, *RAKE: A simple and efficient lossless compression algorithm for the internet of things*, in 2017 25th European Signal Processing Conference (EUSIPCO), 2017, p. 2581–2585.
- [17] D. R. CANTERLE, T. L. DA SILVEIRA, F. M. BAYER, AND R. J. CINTRA, *A multiparametric class of low-complexity transforms for image and video coding*, Signal Processing, 176 (2020), p. 107685.
- [18] D. F. CHIPER AND L. T. COTOROBAI, *A novel VLSI algorithm for a low complexity VLSI implementation of DCT based on pseudo circular correlation structures*, in 2020 International Symposium on Electronics and Telecommunications, 2020, p. 1–4.
- [19] R.-L. CHUNG, C.-W. CHEN, C.-A. CHEN, P. A. R. ABU, AND S.-L. CHEN, *VLSI implementation of a cost-efficient Loeffler DCT algorithm with recursive CORDIC for DCT-based encoder*, Electronics, 10 (2021), p. 862.
- [20] R. J. CINTRA AND F. M. BAYER, *A DCT approximation for image compression*, IEEE Signal Processing Letters, 18 (2011), p. 579–582.
- [21] R. J. CINTRA, F. M. BAYER, AND C. TABLADA, *Low-complexity 8-point DCT approximations based on integer functions*, Signal Processing, 99 (2014), p. 201–214.
- [22] R. CLARKE, *Application of sine transform in image processing*, Electronics Letters, 19 (1983), pp. 490–491.
- [23] R. J. CLARKE, *Relation between the Karhunen-Loève and cosine transforms*, IEEE Proceedings F Communications, Radar and Signal Processing, 128 (1981), p. 359–360.

- [24] D. F. COELHO, R. J. CINTRA, AND V. S. DIMITROV, *Efficient computation of the 8-point DCT via summation by parts*, Journal of Signal Processing Systems, 90 (2018), p. 505–514.
- [25] D. F. COELHO, R. J. CINTRA, A. MADANAYAKE, AND S. M. PERERA, *Low-complexity scaling methods for DCT-II approximations*, IEEE Transactions on Signal Processing, (2021), p. 1–1.
- [26] V. A. COUTINHO, R. J. CINTRA, F. M. BAYER, S. KULASEKERA, AND A. MADANAYAKE, *A multiplierless pruned DCT-like transformation for image and video compression that requires ten additions only*, Journal of Real-Time Image Processing, (2015), p. 1–9.
- [27] T. L. DA SILVEIRA, R. S. OLIVEIRA, F. M. BAYER, R. J. CINTRA, AND A. MADANAYAKE, *Multiplierless 16-point DCT approximation for low-complexity image and video coding*, Signal, Image and Video Processing, 11 (2017), p. 227–233.
- [28] S. DOMOUCHTSIDIS, C. G. TSINOS, S. CHATZINOTAS, AND B. OTTERSTEN, *Symbol-level precoding for low complexity transmitter architectures in large-scale antenna array systems*, IEEE Transactions on Wireless Communications, 18 (2019), pp. 852–863.
- [29] J. DONG, K. N. NGAN, C.-K. FONG, AND W.-K. CHAM, *2-D order-16 integer transforms for HD video coding*, IEEE Transactions on Circuits and Systems for Video Technology, 19 (2009), p. 1462–1474.
- [30] D. S. DUMMIT AND R. M. FOOTE, *Abstract algebra*, vol. 3, Wiley Hoboken, 2004.
- [31] R. V. ESCOBAR, A. M. PATIÑO, I. M. MORENO, M. G. RAMÍREZ, E. R. ARCHUNDIA, AND J. A. G. GNECCHI, *Evaluation and comparison of DCT approximations on FPGA for hardware reduction*, in 2020 IEEE International Autumn Meeting on Power, Electronics and Computing, vol. 4, 2020, p. 1–5.
- [32] E. FEIG AND S. WINOGRAD, *Fast algorithms for the discrete cosine transform*, IEEE Transactions on Signal Processing, 40 (1992), p. 2174–2193.
- [33] B. FLURY AND W. GAUTSCHI, *An algorithm for simultaneous orthogonal transformation of several positive definite symmetric matrices to nearly diagonal form*, SIAM Journal on Scientific and Statistical Computing, 7 (1986), p. 169–184.
- [34] R. C. GONZALEZ AND R. E. WOODS, *Digital image processing*, Upper Saddle River, NJ: Prentice Hall, 2012.
- [35] M. B. A. HAGHIGHAT, A. AGHAGOLZADEH, AND H. SEYEDARABI, *Multi-focus image fusion for visual sensor networks in DCT domain*, Computers & Electrical Engineering, 37 (2011), p. 789–797.
- [36] R. HAMZA, A. HASSAN, AND A. S. PATIL, *A lightweight secure IoT surveillance framework based on DCT-DFRT algorithms*, in International Conference on Machine Learning for Cyber Security, Springer, 2019, p. 271–278.
- [37] R. T. HAWHEEL, W. S. EL-KILANI, AND H. H. RAMADAN, *Fast approximate DCT with GPU implementation for image compression*, Journal of Visual Communication and Image Representation, 40 (2016), p. 357–365.
- [38] T. I. HAWHEEL, *A new square wave transform based on the DCT*, Signal Processing, 82 (2001), p. 2309–2319.
- [39] N. J. HIGHAM, *Functions of matrices: theory and computation*, SIAM, 2008.
- [40] H. S. HOU, *A fast recursive algorithm for computing the discrete cosine transform*, IEEE Transactions on Acoustic, Signal, and Speech Processing, 6 (1987), p. 1455–1461.
- [41] S.-F. HSIAO, Y. H. HU, T.-B. JUANG, AND C.-H. LEE, *Efficient VLSI implementations of fast multiplierless approximated DCT using parameterized hardware modules for silicon intellectual property design*, IEEE Transactions on Circuits and Systems I: Regular Papers, 52 (2005), p. 1568–1579.
- [42] A. E. IBHAZE, P. E. ORUKPE, AND F. O. EDEKO, *High capacity data rate system: Review of visible light communications technology*, Journal of Electronic Science and Technology, 18 (2020), p. 100055.
- [43] A. K. JAIN, *Image data compression: A review*, Proceedings of the IEEE, 69 (1981), p. 349–389.
- [44] R. JAIN AND P. JAIN, *FPGA implementation of recursive algorithm of DCT*, in Proceedings of International Conference on Artificial Intelligence and Applications, Springer, 2021, p. 203–212.
- [45] S. JAMMALAMADAKA AND A. SENGUPTA, *Topics in Circular Statistics*, vol. 5 of Series on multivariate analysis, World Scientific, 2001.
- [46] I. JOLLIFFE, *Principal component analysis*, Wiley Online Library, 2002.
- [47] L. KANSAL, G. S. GABA, N. CHILAMKURTI, AND B.-G. KIM, *Efficient and robust image communication techniques for 5G applications in smart cities*, Energies, 14 (2021), p. 3986.

- [48] J. KATTO AND Y. YASUDA, *Performance evaluation of subband coding and optimization of its filter coefficients*, Journal of Visual Communication and Image Representation, 2 (1991), p. 303–313.
- [49] S. KULASEKERA, A. MADANAYAKE, D. SUAREZ, R. J. CINTRA, AND F. M. BAYER, *Multi-beam receiver apertures using multiplierless 8-point approximate DFT*, in 2015 IEEE Radar Conference (RadarCon), IEEE, 2015, p. 1244–1249.
- [50] D.-U. LEE, H. KIM, M. RAHIMI, D. ESTRIN, AND J. D. VILLASENOR, *Energy-efficient image compression for resource-constrained platforms*, IEEE Transactions on Image Processing, 18 (2009), p. 2100–2113.
- [51] K. LENGWEHASATIT AND A. ORTEGA, *Scalable variable complexity approximate forward DCT*, IEEE Transactions on Circuits and Systems for Video Technology, 14 (2004), p. 1236–1248.
- [52] A. LEVITIN, *Introduction To Design And Analysis Of Algorithms, 2/E*, Pearson Education India, 2008.
- [53] J. LIANG AND T. D. TRAN, *Fast multiplierless approximation of the DCT with the lifting scheme*, IEEE Transactions on Signal Processing, 49 (2001), p. 3032–3044.
- [54] W.-D. LIANG AND X.-D. LIU, *Comparison of approximate DCT and approximate DTT for image compression*, in 2021 IEEE 2nd International Conference on Big Data, Artificial Intelligence and Internet of Things Engineering, 2021, p. 337–341.
- [55] Y. LIANG, G. LIU, N. ZHOU, AND J. WU, *Image encryption combining multiple generating sequences controlled fractional DCT with dependent scrambling and diffusion*, Journal of Modern Optics, 62 (2015), p. 251–264.
- [56] S. MA AND P. AMPADU, *Approximate memory with approximate DCT*, in Proceedings of the 2019 on Great Lakes Symposium on VLSI, 2019, p. 355–358.
- [57] Z. MA, T. HU, L. SHEN, W. KONG, AND B. ZHAO, *A detection and relative direction estimation method for UAV in sense-and-avoid*, in 2015 IEEE International Conference on Information and Automation, 2015, p. 2677–2682.
- [58] A. MADANAYAKE, R. J. CINTRA, N. AKRAM, V. ARIYARATHNA, S. MANDAL, V. A. COUTINHO, F. M. BAYER, D. COELHO, AND T. S. RAPPAPORT, *Fast radix-32 approximate DFTs for 1024-beam digital RF beamforming*, IEEE Access, 8 (2020), p. 96613–96627.
- [59] A. MADANAYAKE, R. J. CINTRA, V. DIMITROV, F. BAYER, K. A. WAHID, S. KULASEKERA, A. EDIRISURIYA, U. POTLURI, S. MADISHETTY, AND N. RAJAPAKSHA, *Low-power VLSI architectures for DCT/DWT: Precision vs approximation for HD video, biomedical, and smart antenna applications*, IEEE Circuits and Systems Magazine, 15 (2015), p. 25–47.
- [60] S. K. MADISHETTY, A. MADANAYAKE, R. J. CINTRA, V. S. DIMITROV, AND D. H. MUGLER, *VLSI architectures for the 4-tap and 6-tap 2-D daubechies wavelet filters using algebraic integers*, IEEE Transactions on Circuits and Systems I: Regular Papers, 60 (2012), p. 1455–1468.
- [61] J. MAHER, A. ALFALOU, AND P. K. MEHER, *A generalized algorithm and reconfigurable architecture for efficient and scalable orthogonal approximation of DCT*, IEEE Transactions on Circuits and Systems I: Regular Papers, 62 (2014), p. 449–457.
- [62] J. MAHER AND P. K. MEHER, *Scalable approximate DCT architectures for efficient HEVC-compliant video coding*, IEEE Transactions on Circuits and Systems for Video Technology, 27 (2017), p. 1815–1825.
- [63] K. MARDIA AND P. JUPP, *Directional Statistics*, Wiley Series in Probability and Statistics, Wiley, 2009.
- [64] G. MARGELIS, X. FAFOUTIS, G. OIKONOMOU, R. PIECHOCKI, T. TRYFONAS, AND P. THOMAS, *Efficient DCT-based secret key generation for the internet of things*, Ad Hoc Networks, 92 (2019), p. 101744.
- [65] M. MASERA, G. MASERA, AND M. MARTINA, *An area-efficient variable-size fixed-point DCT architecture for HEVC encoding*, IEEE Transactions on Circuits and Systems for Video Technology, 30 (2020), p. 232–242.
- [66] K. MECHOUEK, N. KOUADRIA, N. DOGHMANE, AND N. KADDECHE, *Low complexity DCT approximation for image compression in wireless image sensor networks*, Journal of Circuits, Systems and Computers, 25 (2016), p. 1650088.
- [67] H. OCHOA-DOMINGUEZ AND K. R. RAO, *Discrete Cosine Transform*, CRC Press, 2019.
- [68] R. S. OLIVEIRA, R. J. CINTRA, F. M. BAYER, T. L. DA SILVEIRA, A. MADANAYAKE, AND A. LEITE, *Low-complexity 8-point DCT approximation based on angle similarity for image and video coding*, Multidimensional Systems and Signal Processing, 30 (2019), p. 1363–1394.
- [69] A. V. OPPENHEIM, *Discrete-time signal processing*, Pearson Education India, 3rd ed., 1999.
- [70] G. PAIM, M. FONSECA, E. COSTA, AND S. ALMEIDA, *Power efficient 2-D rounded cosine transform with adder compressors for image compression*, in 2015 IEEE International Conference on Electronics, Circuits, and Systems (ICECS), 2015, p. 348–351.

- [71] W. B. PENNEBAKER AND J. L. MITCHELL, *JPEG Still Image Data Compression Standard*, Van Nostrand Reinhold, New York, NY, 1992.
- [72] U. POTLURI, A. MADANAYAKE, R. CINTRA, F. BAYER, AND N. RAJAPAKSHA, *Multiplier-free DCT approximations for RF multi-beam digital aperture-array space imaging and directional sensing*, *Measurement Science and Technology*, 23 (2012), p. 114003.
- [73] U. S. POTLURI, A. MADANAYAKE, R. J. CINTRA, F. M. BAYER, S. KULASEKERA, AND A. EDIRISURIYA, *Improved 8-point approximate DCT for image and video compression requiring only 14 additions*, *IEEE Transactions on Circuits and Systems I: Regular Papers*, 61 (2014), p. 1727–1740.
- [74] A. D. POULARIKAS, *Transforms and applications handbook*, CRC press, 2010.
- [75] M. T. POURAZAD, C. DOUTRE, M. AZIMI, AND P. NASIOPOULOS, *HEVC: The new gold standard for video compression: How does HEVC compare with H.264/AVC?*, *IEEE Consumer Electronics Magazine*, 1 (2012), p. 36–46.
- [76] D. PUCHALA, *Approximate calculation of 8-point DCT for various scenarios of practical applications*, *EURASIP Journal on Image and Video Processing*, 2021 (2021), p. 1–34.
- [77] A. PURI, X. CHEN, AND A. LUTHRA, *Video coding using the H. 264/MPEG-4 AVC compression standard*, *Signal processing: Image communication*, 19 (2004), p. 793–849.
- [78] N. RAJAPAKSHA, A. EDIRISURIYA, A. MADANAYAKE, R. J. CINTRA, D. ONEN, I. AMER, AND V. S. DIMITROV, *Asynchronous realization of algebraic integer-based 2D DCT using Achronix Speedster SPD60 FPGA*, *Journal of Electrical and Computer Engineering*, 2013 (2013), p. 1–9.
- [79] K. R. RAO AND P. YIP, *Discrete Cosine Transform: Algorithms, Advantages, Applications*, Academic Press, San Diego, CA, 1990.
- [80] K. R. RAO AND P. YIP, *The transform and data compression handbook*, CRC press, 2001.
- [81] J. J. ROTMAN, *An introduction to the theory of groups*, vol. 148, Springer Science & Business Media, 2012.
- [82] D. SALOMON, G. MOTTA, AND D. BRYANT, *Data Compression: The Complete Reference*, Springer, 2007.
- [83] S. SAPONARA, *Real-time and low-power processing of 3D direct/inverse discrete cosine transform for low-complexity video codec*, *Journal of Real-Time Image Processing*, 7 (2012), p. 43–53.
- [84] K. SAYOOD, *Introduction to data compression*, Morgan Kaufmann, 2017.
- [85] G. A. SEBER, *A matrix handbook for statisticians*, vol. 15, John Wiley & Sons, 2008.
- [86] R. K. SENAPATI, U. C. PATI, AND K. K. MAHAPATRA, *A low complexity orthogonal  $8 \times 8$  transform matrix for fast image compression*, *Proceeding of the Annual IEEE India Conference (INDICON)*, Kolkata, India, (2010), p. 1–4.
- [87] C. SENTHILPARI, M. I. T. NIRMAL RAJ, P. V. KUMAR, AND J. S. FRANCISCA, *Design a low voltage amp; low power multiplier-free pipelined DCT architecture using hybrid full adder*, in *2018 IEEE 5th International Conference on Engineering Technologies and Applied Sciences (ICETAS)*, 2018, p. 1–6.
- [88] T. SHELTAMI, M. MUSADDIQ, AND E. SHAKSHUKI, *Data compression techniques in wireless sensor networks*, *Future Generation Computer Systems*, 64 (2016), p. 151–162.
- [89] Y. Q. SHI AND H. SUN, *Image and video compression for multimedia engineering: Fundamentals, algorithms, and standards*, CRC press, 1999.
- [90] N. SIDATY, W. HAMIDOUICHE, O. DÉFORGES, P. PHILIPPE, AND J. FOURNIER, *Compression performance of the versatile video coding: HD and UHD visual quality monitoring*, in *2019 Picture Coding Symposium (PCS)*, 2019, p. 1–5.
- [91] A. SINGHADIA, M. MAMILLAPALLI, AND I. CHAKRABARTI, *Hardware-efficient 2D-DCT/IDCT architecture for portable HEVC-compliant devices*, *IEEE Transactions on Consumer Electronics*, 66 (2020), p. 203–212.
- [92] G. STRANG, *Linear Algebra and Its Applications*, Brooks Cole, Feb. 1988.
- [93] H. SUN, Z. CHENG, A. M. GHAREHBAGHI, S. KIMURA, AND M. FUJITA, *Approximate DCT design for video encoding based on novel truncation scheme*, *IEEE Transactions on Circuits and Systems I: Regular Papers*, 66 (2019), p. 1517–1530.
- [94] H. SURESH, S. HEGDE, AND J. SARTORI, *Approximate compression: enhancing compressibility through data approximation*, in *Proceedings of the 15th IEEE/ACM Symposium on Embedded Systems for Real-Time Multimedia*, 2017, p. 41–50.

- [95] T. SUZUKI AND M. IKEHARA, *Integer DCT based on direct-lifting of DCT-IDCT for lossless-to-lossy image coding*, IEEE Transactions on Image Processing, 19 (2010), p. 2958–2965.
- [96] C. J. TABLADA, F. M. BAYER, AND R. J. CINTRA, *A class of DCT approximations based on the Feig–Winograd algorithm*, Signal Processing, 113 (2015), p. 38–51.
- [97] C. THIRIPURASUNDARI, V. SUMATHY, AND C. THIRUVENGADAM, *An FPGA implementation of novel smart antenna algorithm in tracking systems for smart cities*, Computers & Electrical Engineering, 65 (2018), p. 59–66.
- [98] I. TSOUNIS, A. PAPADIMITRIOU, AND M. PSARAKIS, *Analyzing the impact of approximate adders on the reliability of FPGA accelerators*, in 2021 IEEE European Test Symposium, 2021, p. 1–2.
- [99] USC-SIPI, *The USC-SIPI image database*, 2017.
- [100] L. VAN DER PERRE, L. LIU, AND E. G. LARSSON, *Efficient DSP and circuit architectures for massive MIMO: State of the art and future directions*, IEEE Transactions on Signal Processing, 66 (2018), pp. 4717–4736.
- [101] K. WAHID, S.-B. KO, AND D. TENG, *Efficient hardware implementation of an image compressor for wireless capsule endoscopy applications*, in 2008 IEEE International Joint Conference on Neural Networks, IEEE, 2008, p. 2761–2765.
- [102] K. A. WAHID, M. A. ISLAM, AND S.-B. KO, *Lossless implementation of Daubechies 8-tap wavelet transform*, in 2011 IEEE International Symposium of Circuits and Systems, IEEE, 2011, p. 2157–2160.
- [103] G. K. WALLACE, *The JPEG still picture compression standard*, IEEE Transactions on Consumer Electronics, 38 (1992), p. 18–34.
- [104] Z. WANG AND A. C. BOVIK, *Mean squared error: Love it or leave it? A new look at signal fidelity measures*, IEEE Signal Processing Magazine, 26 (2009), p. 98–117.
- [105] Z. WANG, A. C. BOVIK, H. R. SHEIKH, AND E. P. SIMONCELLI, *Image quality assessment: from error visibility to structural similarity*, IEEE Transactions on Image Processing, 13 (2004), p. 600–612.
- [106] T. A. WELCH, *A technique for high-performance data compression*, Computer, 17 (1984), p. 8–19.
- [107] P. YIP AND K. RAO, *The decimation-in-frequency algorithms for a family of discrete sine and cosine transforms*, Circuits, Systems and Signal Processing, 7 (1988), p. 3–19.
- [108] H. J. ZASSENHAUS, *The theory of groups*, Courier Corporation, 2013.
- [109] Y. ZENG, H. SUN, J. KATTO, AND Y. FAN, *Approximated reconfigurable transform architecture for VVC*, in 2021 IEEE International Symposium on Circuits and Systems (ISCAS), 2021, p. 1–5.
- [110] J. ZHANG, W. SHI, L. ZHOU, R. GONG, L. WANG, AND H. ZHOU, *A low-power and high-PSNR unified DCT/IDCT architecture based on EARC and enhanced scale factor approximation*, IEEE Access, 7 (2019), p. 165684–165691.
- [111] L. ZHANG, W. LI, Y. WU, S. LAFLECHE, Z. HONG, S.-I. PARK, J.-Y. LEE, H.-M. KIM, N. HUR, E. IRADIER, P. ANGUEIRA, AND J. MONTALBAN, *Using layered division multiplexing for wireless in-band distribution links in next generation broadcast systems*, IEEE Transactions on Broadcasting, 67 (2021), pp. 68–82.
- [112] X. ZHAO, S.-H. KIM, Y. ZHAO, H. E. EGILMEZ, M. KOO, S. LIU, J. LAINEMA, AND M. KARCZEWICZ, *Transform coding in the VVC standard*, IEEE Transactions on Circuits and Systems for Video Technology, 31 (2021), pp. 3878–3890.
- [113] N. ZIDANI, N. KOUADRIA, N. DOGHMANE, AND S. HARIZE, *Low complexity pruned DCT approximation for image compression in wireless multimedia sensor networks*, in 2019 5th International Conference on Frontiers of Signal Processing (ICFSP), 2019, p. 26–30.